MECHANICAL DAMPER STUDY FOR ISAC-II QUARTER WAVE RESONATORS

L. Yang, V. Zvyagintsev, R.E. Laxdal, TRIUMF, Vancouver, Canada

Abstract

ISAC-II superconducting quarter wave resonators are equipped with mechanical dampers to supress mechanical oscillations of the cavity structure. The study has been carried out to optimize the damper efficiency.

INTRODUCTION

The mechanical oscillation of inner conductor is an essential cause of instability of superconducting coaxial quarter wave resonators (QWR). Due to its low resonant frequency, the fundamental mechanical mode could be easily excited by helium pressure fluctuation, vacuum pumping system, vibrations coupled into the helium bath and ambient vibrations. Under natural damping, the intrinsic quality factor could be as high as several hundred with large amplitude of oscillation and long decay time once the mode is built up. It could cause significant frequency detuning and finally could trip the cavity from amplitude and phase locked operating regime. The ISAC-II linac at TRIUMF has 40 superconducting QWRs: 20 cavities operating at 106 MHz and 20 at 141 MHz. In order to reduce the detuning effect from mechanical oscillations, a kind of dry friction-based mechanical damper designed in INFN-LNL [1], is employed in all the ISAC-II QWRs [2]. The damper is dissipating oscillation kinetic energy by means of friction. ISAC-II operates with negligible beam loading and to operate in locked amplitude and phase loop regime overcoupling is required to provide loaded cavity bandwidth significantly higher than frequency detuning from mechanical oscillations.106 MHz QWR operates for effective accelerating voltage 1 MV and dissipates about 7 W of RF power at 4 K, forward power in overcoupled regime required for stable operation is about 200 W. Such a way the transmission line operates in standing wave regime; most of the RF power is reflecting from the cavity and dissipates in the circulator RF load outside of the cryomodule, at room temperature. Anyway standing wave regime potentially could develop overheat in high current and RF discharge in high voltage locations of the transmission line and coupler. Consequently, it could cause transmission line failure. To mitigate this problem we need to use more expensive components for transmission line: cables, connectors, feedthroughs. The mechanical damper helps to reduce the required overcoupling and RF forward power for the cavities. Study is motivated with possibly to improve the damper efficiency and further reduction of the RF power, which will increase reliability of cryomodule operation. This paper will present the analytical model and experimental results.

THE LOWEST MECHANICAL MODE

The lowest mechanical mode of a QWR is associated with the first order of transverse vibration mode of its inner conductor. Its eigenfrequency and mode vector, could be approximately predicted by a model known as cantilever beam [3], and given by the analytic formulas:

$$\omega = \frac{\alpha^2}{L^2}\sqrt{\frac{EI}{\rho A}}$$

$$\phi(z,L) = \frac{1}{2}\left[cosh\left(\alpha\frac{z}{L}\right) - cos\left(\alpha\frac{z}{L}\right) - 0.734\left\{sinh\left(\alpha\frac{z}{L}\right) - sin\left(\alpha\frac{z}{L}\right)\right\}\right]. \quad (1)$$

Here, E, L, I, ρ, A, stand for the beam's Young modulus, length, geometrical moment of inertia, mass density, cross area, and α is the mode constant; for the first mode $\alpha = 1.875$. For 106 MHz QWR parameters the formula predicts the result of 83.5 Hz. This model doesn't take into account the shorting plate extension, hence, the eigenfrequency is actually overestimated. The finite element method by using ANSYS is able to do the modal calculation for the entire 3D model [4], and predicts the frequency 68 Hz.

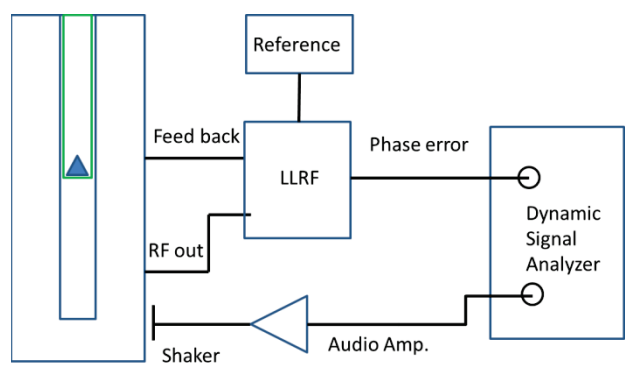

Figure 1: Schematic of setup for mechanical mode measurements.

Measurements at room temperature have been done to verify the simulation results. Figure 1 shows the schematic of setup, which was also used for the later damper measurement. A mechanical shaker driven by an audio amplifier is used to induce the vibration of the 106MHz ISAC-II QWR. The LLRF board operating in the general driven mode provides phase error signal induced by the cavity detuning regarding to reference frequency due to vibration. Reference frequency is tuned for the cavity resonance. The Dynamic Signal Analyzer (DSA) processes the phase error signal by FFT, and provides the spectrum of the cavity's response to the shaker. DSA also provides a sinusoidal drive signal to the

Copyright © 2015 CC-BY-3.0 and by the respective authors

audio amplifier. The resonant curve of the cavity mechanical modes was obtained by sweeping the drive signal frequency (Figure 2 a). There are two peaks split at 68 Hz because of axial asymmetry introduced by the drift tube.

To define mechanical mode quality factor we used phase error signal to measure the decay time after turning off the shaker vibrating at a steady state (Figure 2 b). Fitting the envelope yields the quality factor 378, corresponding to the natural damping ratio 0.0013.

a.

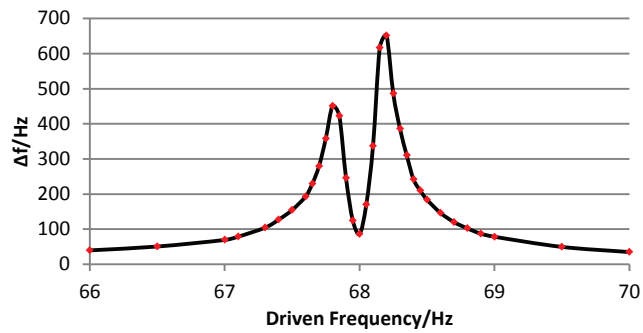

b.

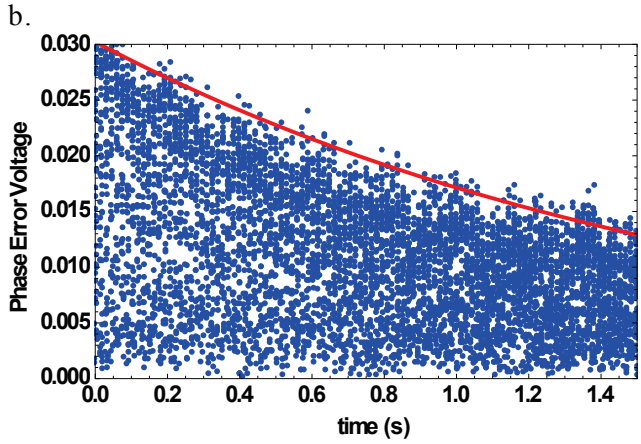

Figure 2: a. Frequency response; b. Decay time measurement.

MODEL DEVELOPMENT

The mechanical damper consists of three parts: a brass load cone, a stainless steel dissipator cone, and three pins, as shown in Figure 3a. The load cone provides the main normal pressure acting on the dissipater cone, which sits on a brass terminating disk at the bottom of a reinforce tube. The pins are evenly azimuthally distributed to transfer the motion of the inner conductor to the dissipater cone. The whole system could be mathematically described by an equivalent mass-spring model. In order to study the damper's performance, a harmonic drive is added to the system. Figure 3b shows the equivalent mass-spring model with the following dimensionless quantities defined:

$$\epsilon = \frac{m_2}{m_1}, p = \frac{k_2}{k_1}, f = \frac{F}{\phi_d \mu N}, f_N = \frac{F_N}{\phi_d \mu N}, \omega_1^2 = \frac{k_1}{m_1}, \Omega = \frac{\omega}{\omega_1}$$

$$u = \frac{k_1 U}{\phi_d \mu N}, y = \frac{k_1 Y}{\phi_d \mu N}, t = \omega T, \xi_1 = \frac{c_1}{2\sqrt{k_1 m_1}}, \xi_2 = \frac{c_2}{2\sqrt{k_2 m_2}}$$

where μ is the sliding friction coefficient (assuming it is the same as the maximum static friction coefficient), N is the normal force, and ϕ_d is the mode vector at the damper's location. Here, the tip motion of the reinforce tube is scaled up to that of the inner conductor with the scale factor ϕ_d.The spring constant of the lowest mode is described by the formula [3]:

$$k = \frac{\alpha^4}{4}\frac{EI}{L^3} \tag{2}$$

The relation, $m = k/\omega^2$, determines the mass constant. The eigenfrequency could be calculated in advance from ANSYS simulation or from measurements.

a.

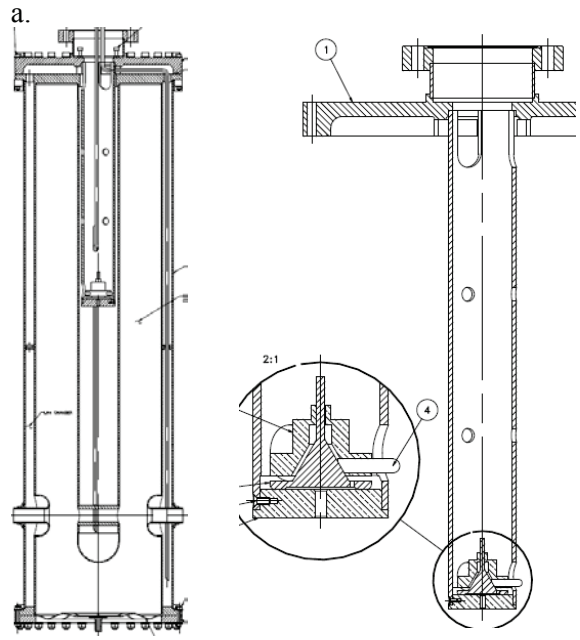

b.

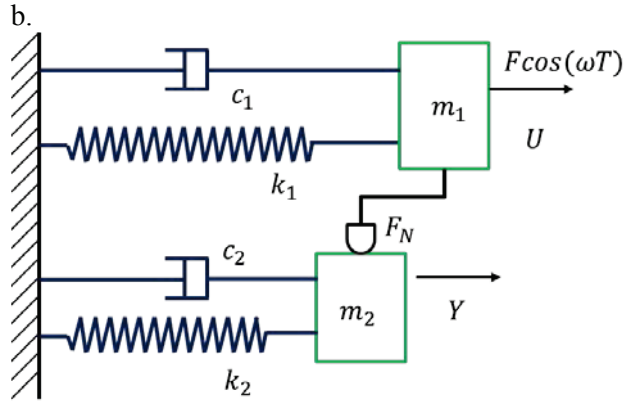

Figure 3: a. Design of the 106 MHz QWR and damper assembly; b. Equivalent spring-mass model.

The system is governed by two equations of motion:

$$\begin{aligned} u'' + 2\xi_1 u' + u &= f cos(\Omega t) - f_N \\ \epsilon y'' + 2\xi_2 \epsilon p y' + p y &= f_N \end{aligned} \tag{3}$$

Due to the nonlinear effect of friction, the damping efficiency highly depends on the drive, and analytic

Copyright © 2015 CC-BY-3.0 and by the respective authors

ISBN 978-3-95450-178-6

solution is not applicable for such a kind of equations. The purpose of this model development is not an accurate solution but interpretation of the physics behaviour of the system. Because of the friction, the inner conductor is mechanically coupled with the reinforce tube. When the drive is relatively low to overcome the maximum static friction, the inner conductor and the reinforce tube are bundled in a common mode. The common mode has higher eigenfrequency than the first mode of the inner conductor. Increasing the drive force would eventually trigger the relative motion between the inner conductor and the reinforce tube. The damper starts to slip since the common mode couldn't be maintained any more, meanwhile, the response stops to increase linearly with the drive. The damper slips and sticks partially, and the slip rate over a period depends on the drive level. The co-existence comes to the end with that the damper could freely slip when the drive is so large. The motion now is dominated by the inner conductor, and the resonance occurs approximately at its natural frequency. Based on the damper's response to the drive, the equation set could be separately solved if only looking at the maximum response.

I. The equation of motion for two bundled harmonic oscillators:

$$(1+\epsilon)u'' + 2(\xi_1 + \xi_2\epsilon p)u' + (1+p)u = f\cos(\Omega t) \tag{4}$$

The common mode is on resonance at $\Omega^2 = \Omega_1^2 = \frac{1+p}{1+\epsilon}$, corresponding to the maximum response,

$$u = \frac{f}{2(\xi_1 + \xi_2\epsilon p)\Omega_1} \tag{5}$$

The turn point (f_1, u_1) where sliding starts at is determined by:

$$pu_1 - \epsilon u_1\Omega_1^2 = 1$$
$$u_1 = \frac{f_1}{2(\xi_1 + \xi_2\epsilon p)\Omega_1} \tag{6}$$

II. The common mode collapses and the damper slips partially. The solution could be linearly approximated by the start point $(f_1, u_1)$and the end point (f_2, u_2), then slip occurs even it is driven at the inner conductor's natural frequencyω_1 $(\Omega = \Omega_2 = 1)$:

$$pu_2 - \epsilon u_2\Omega_2^2 = 1$$
$$u_2 = \frac{f_2}{\sqrt{(\epsilon - p)^2 + [2(\xi_1 + \xi_2\epsilon p)]^2}} \tag{7}$$

III. The damper freely slips over the bottom disk. A method of equivalent viscous damping is adopted to represent the friction damping [5]. The motion is dominated by the inner conductor, therefore the equation set becomes:

$$u'' + 2(\xi_1 + \xi_d)u' + u = f\cos(\Omega t) \tag{8}$$

where $\xi_d = \frac{2}{\pi u}$, is the equivalent viscous damping ratio. The response on resonance is given by

$$u = \frac{f}{2(\xi_1 + \xi_d)\Omega_3}, \Omega_3 = 1 \tag{9}$$

With an algebraic simplification, the solution may be written as,

$$u = \frac{f - \frac{4}{\pi}}{2\xi_1} \tag{10}$$

For the real solution, $f > 4/\pi$. Here one can set the start point f_3 slightly over $4/\pi$, for instance, 20%. The gap between f_2 and $f_3$also could be linearly approximated.

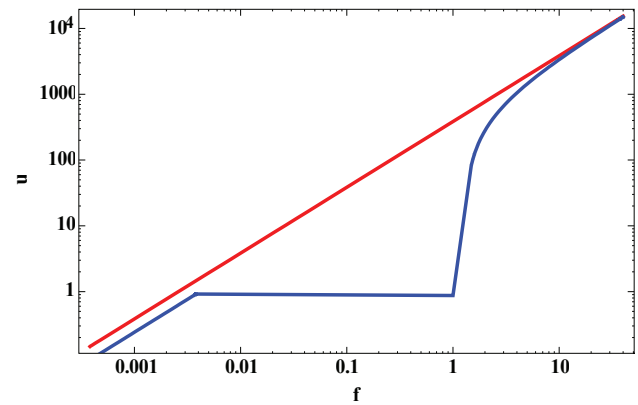

Figure 4: Numerical result of Eq. 3, with (blue) and without (red) damper. The parameters used for evaluation: $k_1 = 1.54e5$ N/m , $m_1 = 0.84$kg , $\epsilon = 0.046$, $p = 1.2$, $\phi_d = 0.36$, $\mu N = 0.648$, $\xi_1 = 0.0013$, $\xi_2 = 0.002$ [6].

The numerical result is depicted in Figure 4 with the parameters used for evaluation. The resonant response without damper, known as $(f/2\xi_1)$, is added to the plot as well to better illustrate the damping efficiency. Interestingly, the partial slips stage provides the most effective damping, where the common mode could be easily destroyed due to sliding triggered at the beginning of the mode building up. On the other hand, the inner conductor' first mode is suppressed by friction. It turns out that neither of the two modes could be completely excited, hence a mix state of stick and slip appears and presents a platform on the plot. Apparently, the sliding friction determines how much drive is able to destroy the common mode. For better sensitivity, one has to reduce the damper load or the friction coefficient, and the reverse way would increase the effective damping range but certainly lose sensitivity. The fully stick stage in the common mode with the enhanced stiffness and added damping ratio, ξ_2 , however, still provides somewhat damping. As for the freely slip stage, the damping efficiency degrades drastically with increasing drive, ending with negligible friction against the large displacement of the inner conductor.

TRANSIENT SIMULATION

Transient simulation has been done with ANSYS transient solver. Neglecting the asymmetry of the drift tube, a simplified 2D model is applicable. Beam element with assigned cross section is selected to model the inner

Copyright © 2015 CC-BY-3.0 and by the respective authors

conductor and the reinforce tube, which connected by a contact element being capable of dry friction issue to represent the damper, referred to CONTAT12. Mass element is added at the end of the inner conductor to tune its natural frequency to the measured number 68 Hz. The simplified model largely reduces the massive meshes of the full 3D model to only 30 meshes, which enables the possibility of transient analysis on an office PC. Harmonic driving force is applied to the inner conductor tip. Multiple runs are required for sweeping over a wide range of drive. The tip displacement of the inner conductor as an indication of the maximum response is observed. Figure 5 shows both the simulation result and the analytical result converted from the dimensionless data in Figure 4. Good agreement on the trend and turn points can be seen from the plot, however, the analytical result overestimated the damping effect somewhat in the partial slips stage possibly due to the sliding in simulation starts a bit later than the analytical prediction, (f_1, u_1). Figure 6 indicates the damping performance of the partial slips stage displayed in the frequency domain. With the damper installed, a flat top is chopped from a sharp resonant peak which originally exists in the common mode. Over the full range of drive, the damper gradually reaches the final freely slip state from the initial stick state. The evolutionary process is well demonstrated in the series of plots at different drive in Figure 7. The slip rate comes to the maximum while the reinforce tube is keeping static.

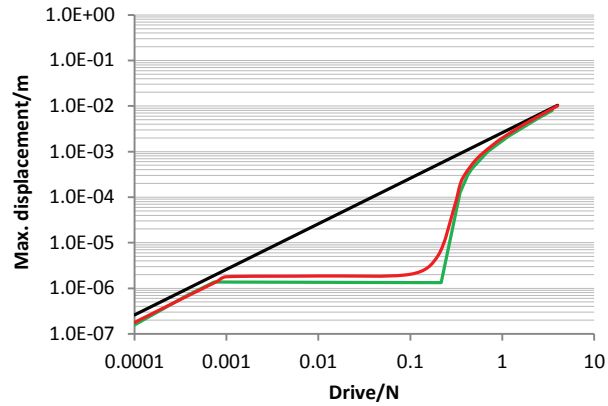

Figure 5: Simulation (red) and analytical (green) result with damper installed, without damper (black).

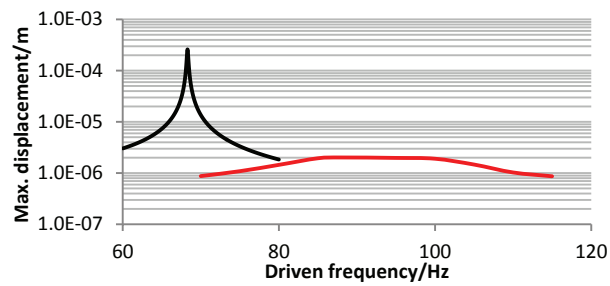

Figure 6: Frequency sweeping at drive of 0.1N, with damper (red), without damper (black).

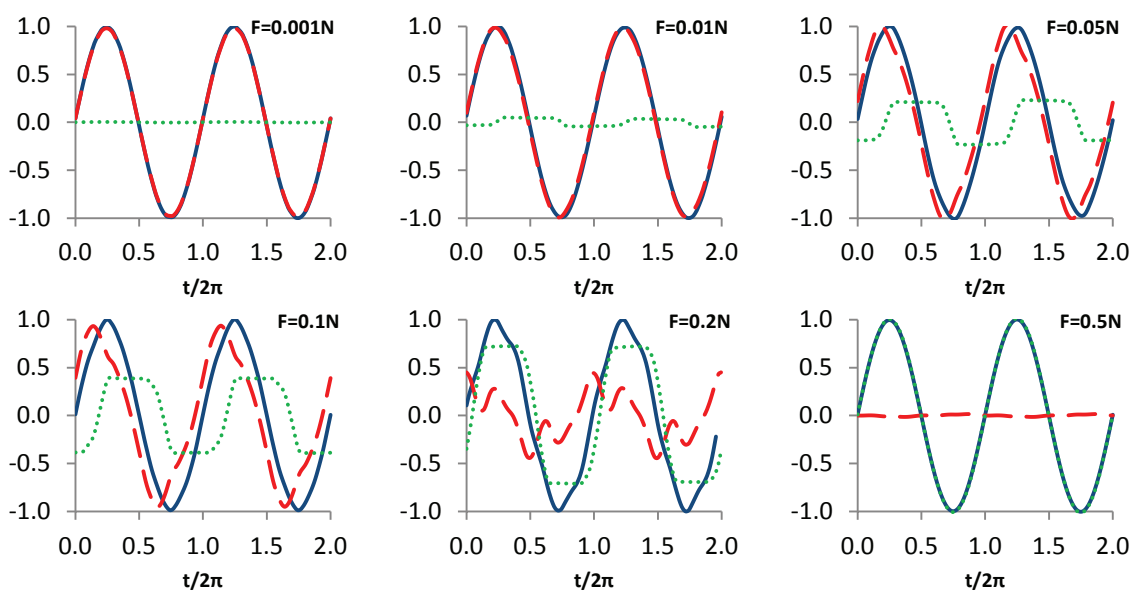

Figure 7: Normalized displacements of the inner conductor (Blue), the reinforce tube (Red) at the damper's location, and their relative motion (Green) varies in a period at different drives.

EXPERIMENT

With the same setup as shown in Figure 1, room temperature measurement was taken first for the 106 MHz QWR without damper as a baseline. The drive for the shaker was swept over a wide range of 3 orders of magnitude to cover all the predicted stages. At a certain drive level, the maximum response was searched with frequency sweeping. Dampers with different weight were installed and measured orderly without interruption of the mechanical setup. The original damper made from brass had a weight of 120 g. Then we prepared a lighter damper of 85 g and aluminium damper of 60 g. We kept the same

Copyright © 2015 CC-BY-3.0 and by the respective authors

ISBN 978-3-95450-178-6

shapes and materials of all contact surfaces. Figure 8 shows the results for all 3 damper loads in comparison to that without damper. Increasing the drive, the damper also goes through 3 stages as the analytical model predicted. The result clearly suggests that lighter damper has better sensitivity but less damping range. The frequency sweeping in Figure 9 indicates a similar chopped-up effect of Figure 6.

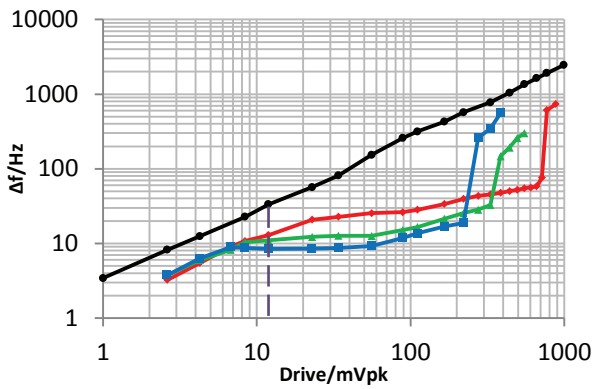

Figure 8: Measurement of drive sweeping without damper (black), with original 120 g damper (red), 85 g damper (green), 60 g damper (blue). The dashed line marks the operational point.

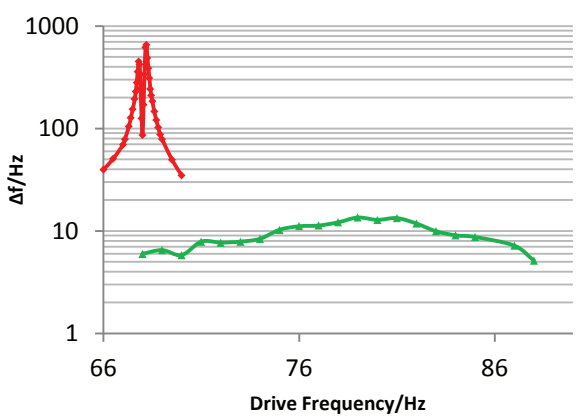

Figure 9: Frequency sweeping at the drive of 221 mVpk, no damper (red), with damper (blue).

The operational half bandwidth for ISAC-II 106 MHz QWRs is typically about 12 Hz, even higher up to 20 Hz, which is supposed to cover the microphonics rms level with sufficient margin. Mapping to the plot in Figure 8, the typical operational point marked with dash line is in the far left range, where the damper sticks to the reinforce tube. The damping comes from the stiffening effect of the reinforce tube as well as its higher intrinsic damping ratio. It only reduces the detuning level by a factor of about 2. The damper may start to work in terms of sudden impacts which contribute the peak level of microphonics. Apparently, ISAC-II 106 MHz QWRs need the damper working with higher sensitivity but with less effective damping range. Cutting off the damper's weight is a simple way to improve the sensitivity. The 60 g damper has shifted the operational point into the effective damping range, where the detuning level is reduced by 35%. Less overcoupling with only a half bandwidth of 8.4 Hz is required, corresponding to a smaller forward power of 139 W. The lightest weight with the friction coefficient kept could be expected is about 45 g by modifying the original design, while the effective range speculated from the Figure 8 won't lose too much to cover the peak level of microphonics, and the required forward power would be further reduced to 86 W with 57% reduction to the current level 200 W.

CONCLUSION

Both analytical and experimental results suggest that the damper works effectively when it partially slips. Lighter damper is able to work more sensitively, but easier to lose the damping efficiency for large vibration. The dampers installed in ISAC-II QWRs are not operating in the effective range due to the heavy load. Reducing the damper's weight is the straightforward way to move its operational point into the effective damping range. One third of the weight could be gotten by modifying the original design with the expected reduction of the forward power by 57%. Further measurement on cryomodule with modified damper installed is required to verify the performance.

ACKNOWLEDGMENT

Great mechanical support of Bhalwinder Waraich on measurement setup and damper machining, inspired discussion with Zhongyuan Yao, and assistance of Norman Muller and Bill Rawnsley are gratefully acknowledged.

REFERENCES

[1] A. Facco, "Mechanical Mode Damping in Superconducting low β resonators", Proc. SRF'97, Padova, Italy, 685 (1997).
[2] R.E. Laxdal, "Production and Testing of Two 141 MHz PrototypeQuarter Wave Cavities for ISAC-II", Proc. LINAC08, Victoria, Canada (2008).
[3] J. Kokavecz, A. Mechler, Phys. Rev. B 78, 172101 (2008).
[4] ANSYS website: http://ansys.com
[5] S. S. Rao, *Mechanical Vibrations*, (Prentice Hall, 2010).
[6] T. Irvine, "Damping properties of materials", November, 2004.

Copyright © 2015 CC-BY-3.0 and by the respective authors